The stress dependence of acoustic properties of heavily doped n-type Ge

1991 J. Phys.: Condens. Matter 3 4547

(http://iopscience.iop.org/0953-8984/3/25/004)

J. Phys.: Condens. Matter 3 (1991) 4547–4553. Printed in the UK

The stress dependence of acoustic properties of heavily doped n-type Ge

H Watanabe, T Sota and K Suzuki
Department of Electrical Engineering, Waseda University, Shinjuku, Tokyo 169, Japan

Received 17 December 1990

Abstract. We calculate the uniaxial stress dependence of the acoustic properties of heavily doped n-type Ge at low temperatures using Green function techniques. It is shown that the results are consistent with experiments of Sb-doped Ge made previously provided that Fermi levels lie in the impurity band. A brief discussion of the magnetic field dependence is also given.

1. Introduction

A series of experimental studies has been done on the acoustic properties of Sb-doped Ge (Sakurai and Suzuki 1983a, b, Sakurai *et al* 1984, Asano *et al* 1988, Kohno *et al* 1988). The experimental data have been analysed in a phenomenological way, namely using the change in the elastic constant by the electron–phonon interaction (see, e.g., Keyes 1968) for $N \gtrsim N_C$ where N is the donor concentration and N_C is the critical concentration for a metal-to-non-metal transition. However, we cannot always analyse the stress and the magnetic field dependence of the ultrasonic attenuation coefficient α using a phenomenological expression in many-valley semiconductors such as Ge and Si.

In this paper we derive expressions for α and the change Δv in the velocity of sound of heavily doped n-type Ge under the uniaxial stress using Green function techniques. Numerical calculations are carried out for Sb-doped Ge and compared with experiment. Our theory can explain the experiment provided that the Fermi levels lie in the impurity band.

2. Formulation

2.1. Preliminary remarks

The conduction band of Ge has four equivalent valleys along the $[111]$, $[\bar{1}1\bar{1}]$, $[1\bar{1}\bar{1}]$ and $[\bar{1}\bar{1}1]$ directions in the first Brillouin zone, which are denoted by valley indices 1, 2, 3 and 4, respectively. The electron–phonon interaction is due to the deformation potential coupling. For high carrier concentrations, acoustic waves accompanied by strains destroying the equivalence of valleys give rise to the redistribution of electrons among valleys and are strongly attenuated. In this case, phenomenological expressions for the attenuation coefficient α and the change Δv in the velocity of sound for $\omega\tau_2 \ll 1$

are proportional to $\Delta C\, \tau_2$ and ΔC, respectively, where ω is the angular frequency of acoustic waves, τ_2 the intervalley scattering time and ΔC the change in the elastic constant caused by the valley redistribution effect.

Previously we have derived formal expressions for α and Δv based on a microscopic theory in heavily doped many-valley semiconductors with n equivalent valleys (Sota and Suzuki 1986, hereafter referred to as I). The procedure for calculations given in this paper is parallel to that given in I except for taking account of the effects of uniaxial stress X and the magnetic field B. In the calculations given below we assume that

(i) only the intravalley processes of the deformation potential coupling are considered because the distance in k-space between different valleys is much larger than the phonon wavevector q of interest to us;
(ii) the electron–phonon coupling in the impurity band is identical with that in the conduction band;
(iii) the effect of the electron correlation on the electron distribution function is neglected and;
(iv) the long-wavelength and the low-frequency region are considered.

Expressions for α and Δv for acoustic waves in the mode (q, λ) are obtained, respectively, from the imaginary and the real parts of the phonon self-energy, which is calculated from the electronic polarization diagram with the electron–phonon interaction vertices, and are as follows:

$$\alpha = -\frac{\omega}{\rho_{\mathrm{m}} v_\lambda^3} \mathrm{Im}\left(\sum_{ij} C^*_{i,q\lambda} R_{ij}(q, \omega) C_{j,q\lambda} \right) \tag{1}$$

and

$$\Delta v = \frac{1}{2\rho_{\mathrm{m}} v_\lambda} \mathrm{Re}\left(\sum_{ij} C^*_{i,q\lambda} R_{ij}(q, \omega) C_{j,q\lambda} \right) \tag{2}$$

where ρ_{m} is the crystal density, v_λ is the velocity of sound with the polarization direction λ, $C_{i,q\lambda}$ is the deformation potential constant in the ith valley and $R_{ij}(q, \omega)$ are the density response functions of the electron subsystem.

Within the random-phase approximation, $R_{ij}(q, \omega)$ are determined by

$$R_{ij}(q, \lambda) = \chi_{ij}(q, \omega) + V(q) \sum_{lm} \chi_{il}(q, \omega) R_{mj}(q, \omega). \tag{3}$$

Here $v(q) = 4\pi e^2/\varepsilon_0 q^2$ and $\chi_{ij}(q, \omega)$ are the irreducible density response functions defined by

$$\chi_{ij}(q, \omega) = 2 \sum_{\varepsilon_n} \sum_{k} \langle G_i(k + q, \varepsilon_n + \omega) G_j(k, \varepsilon_n) \rangle \tag{4}$$

where ε_0 is the static dielectronic constant, $\langle\ \rangle$ stands for the average over the random configuration of impurities and $G_i(k, \varepsilon_n)$ are the single-particle Green function in valley i. Equation (4) is calculated from a series of diagrams shown in figure 1 where the full lines represent the single-particle Green function, the open circle and cross denote the intravalley and intervalley scattering, respectively, and the indices i, j, l and m are valley

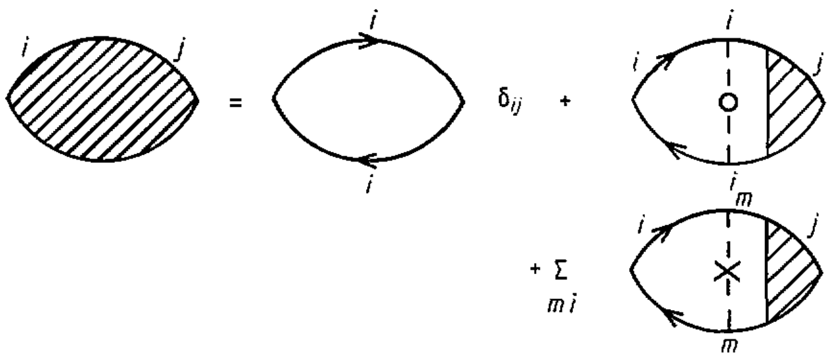

Figure 1. Diagrammatic representation of the irreducible density response functions $\chi_{ij}(q, \omega)$: ——, electron Green functions: --O--, intravalley scattering; -- × --, intervalley scattering.

indices. For details of the calculation of equation (4) with figure 1, refer to I. Once we obtain $\chi_{ij}(\boldsymbol{q}, \omega)$, we can calculate α and Δv using equations (1)–(3).

$\chi_{ij}(\boldsymbol{q}, \omega)$ consist of complex combinations of τ_0 (the total scattering time), τ_2, ω and the density-of-states functions $\varphi^{(j)}$. Here $\varphi^{(j)}$ are given by

$$\varphi^{(j)} = -\int N^{(j)}(E)\,\frac{\partial f(E, \mu_0)}{\partial E}\,\mathrm{d}E \tag{5}$$

where $N^{(j)}(E) = -(1/\pi)\,\Sigma_k\,\mathrm{Im}[G_j(\boldsymbol{k}, E)]$ are the density of states in valley j and f is the Fermi–Dirac distribution function with the chemical potential μ_0. When a uniaxial stress X or a magnetic field $\boldsymbol{B}$ is applied. $N^{(j)}(E)$ are modified. This leads to the X- or B-dependence of $\chi_{ij}(\boldsymbol{q}, \omega)$ and, consequently, the X- or the B-dependence of α and Δv.

2.2. *Expressions for α and Δv under the uniaxial stress X*

We shall give expressions for α and Δv under the uniaxial compressional stress for the following two configurations, where all phonons are longitudinal: case A, $\boldsymbol{X}//[110]$ and $\boldsymbol{q}//[1\bar{1}1]$; case B, $\boldsymbol{X}//[111]$ and $\boldsymbol{q}//[1\bar{1}0]$.

2.2.1. Case A: $\boldsymbol{X}//[110]$ and $\boldsymbol{q}//[1\bar{1}1]$. The uniaxial compressional stress along the [110] axis lowers valleys 1 and 4 by $\Xi_u X/6C_{44}$ and lifts valleys 2 and 3 by $\Xi_u X/6C_{44}$ in energy (Fritzsche 1960) where $X = |\boldsymbol{X}|$, C_{44} is the elastic stiffness constant and Ξ_u is the shear component of the deformation potential constant. In this case the irreducible density response function matrix has five independent elements as follows: $\chi_{11} = \chi_{44}$, $\chi_{22} = \chi_{33}$, χ_{14}, χ_{23}, $\chi_{12} = \chi_{13} = \chi_{24} = \chi_{34}$ and $\chi_{ij} = \chi_{ji}$. Hereafter we abbreviate $\chi_{ij}(\boldsymbol{q}, \omega)$ to χ_{ij}. The final expressions for α and Δv are given by

$$\alpha_A = -(\omega/\rho_m v_A^3)(8/81)\Xi_u^2\,\mathrm{Im}\,R_A \tag{6}$$

and

$$\Delta v_A = (1/2\rho_m v_A)(8/81)\Xi_u^2\,\mathrm{Re}\,R_A \tag{7}$$

with

$$R_A = \chi_{11} - 4\chi_{12} + \chi_{14} + 5\chi_{22} - 3\chi_{23} - (\chi_{11} + \chi_{14} - \chi_{22} - \chi_{23})^2/(\chi_{11} + 4\chi_{12} + \chi_{14} + \chi_{22} + \chi_{23}). \tag{8}$$

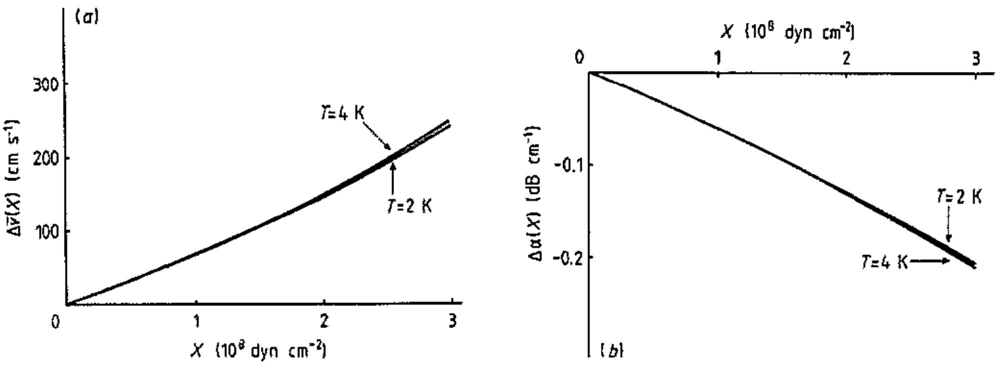

Figure 2. The stress X-dependence of (a) the change $\Delta\bar{v}(X) = \Delta v(X) - \Delta v(0)$ in the velocity of sound and (b) the change $\Delta\alpha(X) = \alpha(X) - \alpha(0)$ in the attenuation constant for $X//[110]$ and $q//[1\bar{1}1]$ at $T = 2$ and 4 K calculated assuming a rigid conduction band.

In equations (5) and (6) the subscript A stands for case A. Explicit expressions for χ_{ij} in this case are given in the appendix.

Here we should mention the following. In equations (6) and (7) we neglect terms with the dilational component Ξ_d of the deformation potential constants. This is because these terms are much smaller than terms in equations (6) and (7) due to the screening effect. This also holds for case B.

2.2.2. Case B: $X//[111]$ and $q//[1\bar{1}0]$. In this case the uniaxial compressional stress lowers valley 1 by $\Xi_u X/3C_{44}$ and lifts the other three valleys by $\Xi_u X/9C_{44}$ in energy (Fritzsche 1962). χ_{ij} have four independent elements: χ_{11}, $\chi_{22} = \chi_{33} = \chi_{44}$, $\chi_{12} = \chi_{13} = \chi_{14}$, $\chi_{23} = \chi_{24} = \chi_{34}$ and $\chi_{ij} = \chi_{ji}$. α and Δv are obtained as follows:

$$\alpha_B = -(\omega/\rho_m v_B^3)\,\tfrac{1}{9}\,\Xi_u^2\,\mathrm{Im}\,R_B \tag{9}$$

and

$$\Delta v_B = (1/2\rho_m v_B)\,\tfrac{1}{9}\,\Xi_u^2\,\mathrm{Re}\,R_B \tag{10}$$

with

$$R_B = \chi_{11} - 2\chi_{12} - 2\chi_{23} + 3\chi_{22} - (\chi_{22} + 2\chi_{23} - 2\chi_{12} - \chi_{11})^2/(\chi_{11} + 3\chi_{22} + 6\chi_{12} + 6\chi_{23}). \tag{11}$$

The subscript B indicates case B. Explicit expressions for χ_{ij} are also given in the appendix.

3. Results

Numerical calculations were carried out for Sb-doped Ge ($N > 2 \times 10^{17}\,\mathrm{cm}^{-3}$) using expressions obtained in section 2 where we used $\rho_m = 5.35\,\mathrm{g\,cm}^{-3}$, $\Xi_u = 16\,\mathrm{eV}$ and $\omega/2\pi = 60\,\mathrm{MHz}$ for Δv and 300 MHz for α. Note that $N_c = 1.5 \times 10^{17}\,\mathrm{cm}^{-3}$ for Sb-doped Ge.

Figure 2 shows $\Delta\bar{v}(X) = \Delta v(X) - \Delta v(0)$ and $\Delta\alpha(X) = \alpha(X) - \alpha(0)$ for case A, $N = 4.6 \times 10^{17}\,\mathrm{cm}^{-3}$ and the rigid, conduction band model. Here $N_0^{(j)}(E) =$

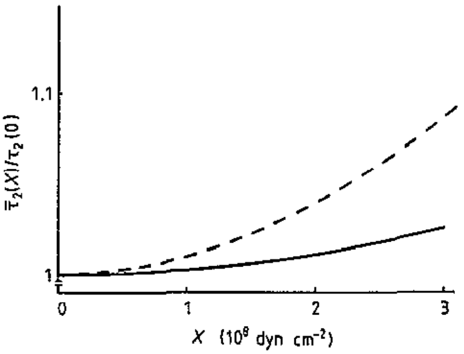

Figure 3. The stress X-dependence of the ratio of the average intervalley scattering time $\bar{\tau}_2(X)$ to $\tau_2(0)$ for $T \ll E_F/k_B$: ——, rigid conduction band; - - -, impurity band.

$(1/2\pi^2)(2m^*/\hbar^2)^{3/2}E^{1/2}$, $m^* = 0.22m_0$, $\tau_0(X=0) = 1 \times 10^{-13}$ s, $\tau_2(X=0) = 4 \times 10^{-11}$ s (Mason and Bateman 1964, Sakurai and Suzuki 1983a) and $v_A = 5.57 \times 10^5$ cm s^{-1} are used. The X-dependence of τ_2 is taken into account via that of $N(E)$ as τ_2 is proportional to $N(E_F)$ for $T \ll E_F/k_B$ where $N(E_F)$ is the density of states at the Fermi energy E_F. The full curve in figure 3 shows the ratio $\bar{\tau}_2(X)/\tau_2(0)$ where $\bar{\tau}_2(X)$ is an average value defined by $\bar{\tau}_2(X) = [\tau_2(1 \to 2, X) + \tau_2(2 \to 1, X)]/2$ and $1 \to 2$ and $2 \to 1$ mean values due to scattering processes from valley 1 to valley 2 and from valley 2 to valley 1, respectively. As N increases, both the X- and the T-dependence of $\Delta\bar{v}(X)$ and $\Delta\alpha(X)$ become weaker. When we neglect the X-dependence of τ_2, the X-dependence of $|\Delta\alpha(X)|$ becomes stronger.

The T-dependence of $\Delta\bar{v}(X)$ shown in figure 2(a) is opposite to experiment where $\Delta\bar{v}(X, T = 2\text{ K}) > \Delta\bar{v}(X, T = 4\text{ K})$ is obtained (Umebayashi and Suzuki 1990). The situation is improved provided that we consider the impurity band instead of the rigid conduction band. A similar phenomenon has been found in a previous paper (Khono *et al* 1988). In fact the T-dependence of $\Delta v(0)$ could not be explained by assuming a rigid conduction band.

Figure 4 shows the results of $\Delta\bar{v}(X)$ and $\Delta\alpha(X)$ calculated for the impurity band whose density of states associated with valley j is given by

$$\hat{N}_0^{(j)}(E) = AE^{1/2}\theta(E) + B\gamma^{1/2}\exp[-\gamma(E - E_0)^2] \tag{12}$$

with $\theta(x) = 1$ for $x > 0$ and $\theta(x) = 0$ for $x < 0$. The adjustable parameters A, B and γ are determined so as to reproduce the T-dependence of $\Delta v(0)$ obtained experimentally over the temperature range $2\text{ K} \leqslant T \leqslant 40\text{ K}$: $A = 1.9 \times 10^{16}$ cm^{-3} meV$^{-3/2}$, $B = 2.2 \times 10^{16}$ cm^{-3} and $\gamma = 2.0$ meV^{-2}. For simplicity, the shape of $\hat{N}_0^{(j)}(E)$ is assumed not to vary with X. The T-dependence of $\Delta\bar{v}(X)$ is consistent with experiment. The X- and the T-dependences of $\Delta\alpha(X)$ are almost unchanged, while the X-dependence of $\bar{\tau}_2(X)/\tau_2(0)$ becomes stronger in comparison with the case of the rigid conduction band (see figure 3).

The behaviours of $\Delta\bar{v}(X)$ and $\Delta\alpha(X)$ in case B are similar to those in case A, but the magnitudes are smaller.

4. Discussion

Phenomenologically α is proportional to $\Delta C\,\bar{\tau}_2$ and Δv to ΔC where $\bar{\tau}_2$ is an average intervalley scattering time. As the stress increases, $|\Delta C|$ decreases, while $\bar{\tau}_2$ increases.

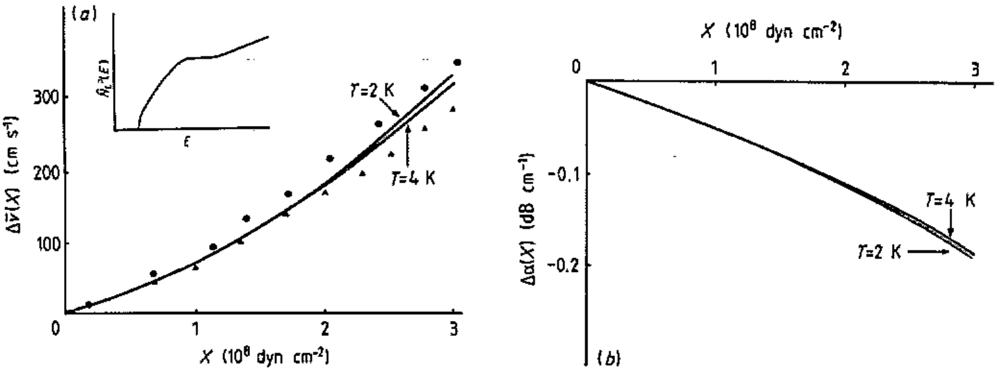

Figure 4. The stress X-dependence of (a) the change $\Delta\bar{v}(X) = \Delta v(X) - \Delta v(0)$ in the velocity of sound and (b) the change $\Delta\alpha(X) = \alpha(X) - \alpha(0)$ in the attenuation constant for $X//[110]$ and $q//[1\bar{1}1]$ at T = 2 and 4 K calculated assuming an impurity band. The inset in (a) shows a schematic illustration of the density of states for the impurity band used in calculations. In (a) the experimental data at T = 2.3 K (●) and 4.2 K (▲) are also shown.

Thus the X-dependences of ΔC and $\bar{\tau}_2$ are partially cancelled in $\Delta\alpha(X)$. The X-dependence is stronger in the impurity band than in the rigid conduction band, which arises from the difference between the energy dependences of $\hat{N}^{(j)}(E)$ and $N^{(j)}(E)$. It was argued in a previous paper (Sakurai and Suzuki 1983b) that $\Delta\alpha(X)$ for $N = 4.6 \times 10^{17}$ cm^{-3} could be quantitatively explained by assuming a rigid conduction band and constant τ_2. However, we find, for this concentration, that $\Delta\alpha(X)$ calculated under this assumption is almost the same as that calculated with $\tau_2(X)$ for the impurity band.

We assumed that the shape or the energy dependence of $N^{(j)}(E)$ did not vary with the stress. It is known from experiments on the piezoresistance (Fritzsche 1962) that the impurity band is modified by the stress for $N \lesssim 2 \times 10^{17}$ cm^{-3} where stresses up to about 10^9 dyn cm^{-2} were used. However, we expect that the shape of $N^{(j)}(E)$ for $N > 2 \times 10^{17}$ cm^{-3} is not varied so much by the stresses up to 3×10^8 dyn cm^{-2} which were used in the acoustic measurements (Sakurai and Suzuki 1983b, Kohno *et al* 1988, Umebayashi and Suzuki 1990) and consequently our calculated results are, at least qualitatively, correct.

Finally we briefly mention the magnetic field dependence of Δv and α. $\Delta\bar{v}(B)$ and $\Delta\alpha(B)$ for B up to 5 T were calculated assuming a rigid conduction band and taking into account collision broadening of Landau levels. As regards $\Delta\bar{v}(B)$ for $N = 4.6 \times 10^{17}$ cm^{-3}, our theory can explain the experiment of Asano *et al* (1988), while the calculated $\Delta\alpha(B)$ are an order of magnitude smaller than experimental values. However, as mentioned above, the impurity band, instead of the conduction band, must be considered for this concentration. We do not know how the wavefunctions and the density of states for the impurity band are modified by the magnetic field.

Appendix

Here we give explicit expressions for χ_{ij} in both case A and case B.

For case A,

$$\chi_{11} = -2\{\varphi^{(1)} - \omega Z_1[2Y_1Y_2 - (X_1 - 1)(X_2 + Y_2 - 1)]/D_1\} \tag{A1}$$

$$\chi_{12} = -2\omega Z_2 Y_1/[Y_2(X_1 - 1) + Y_1(X_2 - 1) + (X_1 - 1)(X_2 - 1) - 3Y_1Y_2] \tag{A2}$$

$$\chi_{14} = -2\omega Z_1 Y_1(Y_2 - X_2 - 1)/D_1 \tag{A3}$$

$$D_1 = (Y_1 - X_1 + 1)[Y_2(X_1 - 1) + Y_1(X_2 - 1) + (X_1 - 1)(X_2 - 1) - 3Y_1Y_2] \tag{A4}$$

$$X_j = -\mathrm{i}2\pi N u^2 N^{(j)}(E_\mathrm{F})Q \tag{A5}$$

$$Y_j = -\mathrm{i}2\pi N v^2 N^{(j)}(E_\mathrm{F})Q \tag{A6}$$

$$Z_j = \varphi^{(j)}Q. \tag{A7}$$

Here the expressions for χ_{22} and χ_{23} are given by interchanging subscripts 1 and 2 in those for χ_{11} and χ_{14}, u and v are the strengths of the intravalley and intervalley scattering potentials, respectively, the subscript j equals 1 or 2, and an explicit expression for $\varphi^{(j)}$ is given by equation (5) in the text.

For case B,

$$\chi_{11} = -2[\varphi^{(1)} - \omega Z_1(2Y_2 + X_2 - 1)/E_1] \tag{A8}$$

$$\chi_{22} = -2\{\varphi^{(2)} - \omega Z_2[-2Y_1Y_2 + (X_2 + Y_2 - 1)(X_1 - 1)]/(X_2 - Y_2 - 1)E_1\} \tag{A9}$$

$$\chi_{12} = -2\omega Z_2 Y_1/E_1 \tag{A10}$$

$$\chi_{23} = -2\omega Z_2 Y_2(Y_1 - X_1 + 1)/(X_2 - Y_2 - 1)E_1 \tag{A11}$$

$$E_1 = (X_1 - 1)(X_2 + 2Y_2 - 1) - 3Y_1Y_2. \tag{A12}$$

Here the expressions for X_j, Y_j, and Z_j $(j = 1, 2)$ are the same as those in equations (A5)–(A7). The function Q appearing in equations (A5)–(A7) is defined by

$$Q \simeq \mathrm{i}\tau_0(1 + \mathrm{i}\omega\tau_0). \tag{A13}$$

References

Asano K, Ogiwara H and Suzuki K 1988 *J. Phys. C: Solid State Phys.* **21** 1477–84
Fritzsche H 1960 *Phys. Rev.* **119** 1899–1900
—— 1962 *Phys. Rev.* **125** 1552–60
Keyes R W 1968 *Solid State Physics* (New York: Academic) pp 37–90
Kohno M, Ogiwara H, Asano K and Suzuki K 1988 *J. Phys. C: Solid State Phys.* **21** 4033–43
Mason W P and Bateman T B 1964 *Phys. Rev.* **134** A 1387–96
Sakurai H and Suzuki K 1983a *J. Phys. Soc. Japan* **52** 4192–8
—— 1983b *J. Phys. Soc. Japan* **52** 4199–205
Sakurai H, Miyasato T and Suzuki K 1984 *J. Phys. Soc. Japan* **53** 1356–9
Sota T and Suzuki K 1986 *Phys. Rev.* B **33** 8458–67
Umebayashi T and Suzuki K 1990 unpublished